



Research Article

Fabricating ultra-sharp tungsten STM tips with high yield: double-electrolyte etching method and machine learning

Bowen Li¹ · Yipeng Zhang¹ · Jiashuai Wang¹ · Zezhao Jia¹ · Chengqian Shi¹ · Yanqing Ma^{1,2}  · Lei Ma¹

Received: 19 December 2019 / Accepted: 9 June 2020
© Springer Nature Switzerland AG 2020

Abstract

The double-electrolyte etching method is a simple and effective way to fabricate ultra-sharp scanning tunnel microscopy (STM) tungsten tips. However, it is still challenging for this method to get ultra-sharp tungsten tips with high yield. In this work, significant enhancing of the yield is presented through optimized etching parameters as follows: temperature of 26 °C, applied voltage 7.5 V, electrolyte concentration 4 mol L⁻¹ and length below the liquid lamellae of 2 mm. Under these conditions, the smallest tip radius is around 8 nm and the yield (radius < 10 nm) is 63.5%. These tips are capable of producing high-quality atomic resolution STM images, as demonstrated by testing on Si (111) and highly oriented pyrolytic graphite (HOPG) samples at room temperature. Furthermore, in order to find the relationship between the tip features and experimental etching parameters, an artificial neural network (ANN) model is built by machine learning. Garson's algorithm is used to analyze the relative importance of each experimental parameter on tip features. The tip features can be estimated by this model with a correlation factor *R* over 0.85 indicating great predictive performance. Importance analysis indicates that the length of the tungsten wire below the liquid lamellae is the most important parameter to obtain high-quality STM tungsten tips in the double-electrolyte etching method. This result provides a clear direction for rapidly selecting optimized tip fabrication parameters in the future.

Keywords Scanning tunnel microscopy · Tungsten tips · Double-electrolyte etching method · Machine learning · Importance analysis

1 Introduction

With the development of nanoscience, there is a growing demand for high-resolution test instruments [1–3]. Scanning tunnel microscopy (STM) that can directly image the surface of samples on the atomic scale has become one of the most powerful measurement techniques for nanoscience [4–8]. The key component of STM is a probe tip which is used to collect the surface information of the sample [9]. And the resolution of the images strongly relies on the tip curvature radius of the probe tip. The smaller the tip curvature radius, the higher the transverse resolution of the

images [10]. However, commercial probes with a tip radius of less than 10 nm are very expensive, and they are so fragile that any contact can damage the tip [11]. Therefore, researchers prefer fabricating ultra-sharp tips in their own laboratory. It has been a long-standing issue to fabricate tips with small radius by a simple and economical method.

Among various tip fabrication methods, direct current (DC) electrochemical etching of tungsten wire is widely used in laboratories because of its advantages of simple fabrication and low cost [12]. But it is challenging for the original DC electrochemical etching method to fabricate tips with radius less than 100 nm. As is known, the key

✉ Yanqing Ma, mayanqing@tju.edu.cn; ✉ Lei Ma, lei.ma@tju.edu.cn | ¹Tianjin International Center for Nanoparticles and Nanosystems, Tianjin University, Tianjin 300072, People's Republic of China. ²State Key Laboratory of Precision Measuring Technology and Instruments, Tianjin University, Tianjin 300072, People's Republic of China.



point of fabricating sharp tungsten tips by DC electrochemical etching method is to cut off the circuit as soon as possible once the tungsten wire breaks; otherwise, the residual current of electrochemical reaction will blunt the tip. The shorter the cutoff time, the smaller the tip radius [13–15]; in the original DC electrochemical etching method the circuit cutoff was controlled manually, which was inefficient and could not get a short enough time to fabricate tips of less than 100 nm. In order to obtain a shorter time, Ibe et al. designed a feedback control circuit based on the sharp drop of the current when the tungsten wire breaks [13]. Through this circuit, probes with tip curvature radius of 20 nm were obtained. Afterward, plenty of efforts have been made to cease the etching circuit more quickly by adding computer monitoring programs and designing more sensitive controls [16–29]. Via these effects, tips with curvature radius less than 10 nm can be fabricated. However, these strategies were too complicated and required the support of sophisticated and expensive electronics. Researchers had to find other ways to avoid the influence of residual current on the tip radius. Lemke et al. [30] used a two-step method and added a non-conductive solution with different densities into conventional electrolytes. Since the lower part of the tungsten wire was out of the etching circuit when the tungsten wire drops, this stub was not affected by residual current and was selected as tip. They also proposed a new technique, named liquid lamellae method, by which spherical tips of 50 nm to 100 nm radii were fabricated. But these lower tips had the issue that their long taper causes mechanical resonance in STM measurements [11]. Klein and Schwitzgebel [31] presented a modified lamellae drop-off scheme for producing a lower tip with more ideal shape. But the tip radius was more than 25 nm and their intermediate inversion operation of tungsten wire complicates the preparation process. Kulawik et al. [32] proposed a double-lamella drop-off etching method that can cut off the circuit automatically in a short time by the weight of the stub when the tungsten wire breaks, whereas the curvature radius of their tungsten tip was still more than 20 nm. Motivated by the urgent need of sharp tungsten tips for use in STM, double-lamella drop-off etching method is explored and further refined. Schoelz et al. [33] adopted the double-lamellae drop-off etching method to fabricate tungsten tips and found the relationship between the tip's cone angle and the possibility of atomically resolved STM images. Based on the same method, Basnet et al. [34] used a simple but effective “etch stop” device to optimize the etching position of the tungsten wire. However, they do not focus on fabricating ultra-sharp tungsten tips. Recently, Li et al. [35] used double-electrolyte etching method to fabricate tungsten

tips with curvature radius less than 10 nm, but the yield was only about 30%, which was not enough to meet the demand for tips in the application.

In this work, high-yield fabrication of ultra-sharp tungsten tips for STM was designed and demonstrated by the double-electrolyte etching method. Moreover, a machine learning method, artificial neural network (ANN), was used to build up the model of tip fabrication under different experimental conditions and distinguish the importance degrees of different parameters that affect the features of the tungsten tips.

2 Experiment

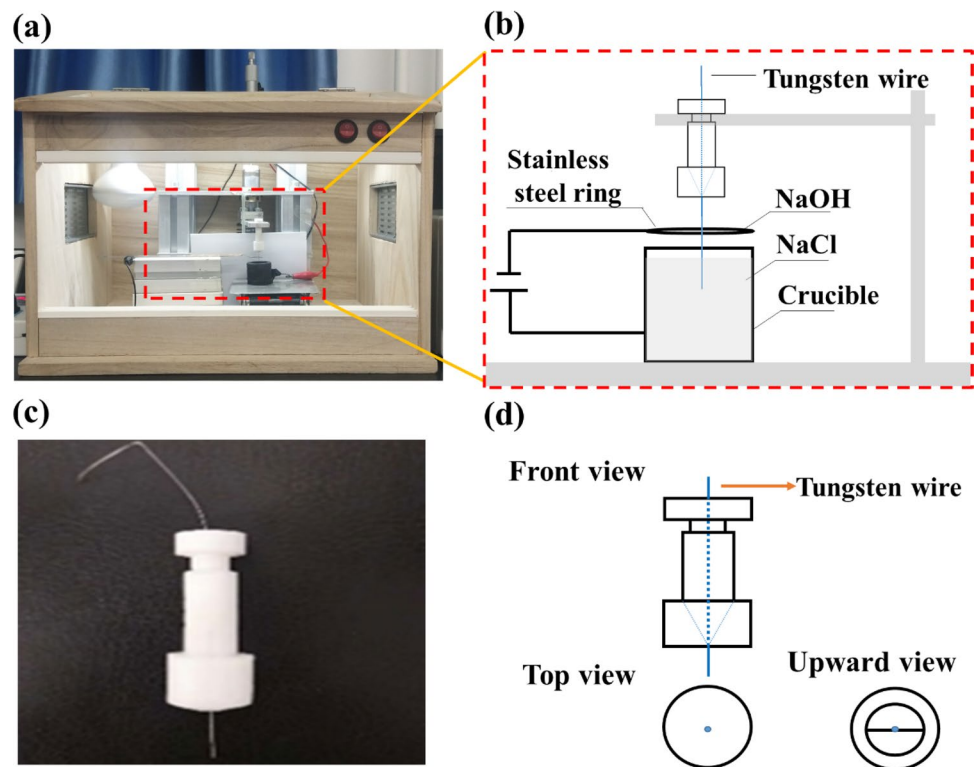
2.1 Experimental details

The experimental setup based on the double lamellae method is shown in Fig. 1a. The full etching circuit and the mechanism behind the double-electrolyte etching method are shown schematically in Fig. 1b. The tungsten wire clamping device is connected with the depth micrometer through a series of linkage devices. The accuracy of the depth micrometer is 0.01 mm so that the length of the tungsten wire (diameter 0.2 mm and 0.25 mm, purity 99.9%, Shuanghua Group Qianchui Metal co., LTD.) below the liquid lamellae can be accurately adjusted. The metal ring used in the experiment is made of stainless steel (diameter 8 mm, thickness 0.3 mm). The liquid lamellae were formed by NaOH (flake, purity 97%, Aladdin) solution. The liquid lamellae must be kept flush with the stainless steel ring before each etching process to ensure the same thickness of the liquid lamellae. The concentrations of NaOH solution used in the experiment were 1, 2, 3, 4 and 5 mol L⁻¹. The crucible contains saturated NaCl (AR, Aladdin) solution. Beneath the crucible is the lifting platform, which can adjust the distance between the tungsten wire and the crucible. The DC power supply (LONG WEI DC Power Supply PS-302D) can provide voltage from 0 to 24 V with electric current precision of 0.01 A.

2.2 Modification of the experimental setup

Several improvements were made to the conventional experimental setup of double-electrolyte etching method: First, a temperature control box was applied to guarantee the entire reaction process proceeds at a stable temperature, which is very important for the etching process. The effects of temperature fluctuation on electrochemical etching reaction will be discussed later. Second, the stainless steel anode was changed into a stainless steel crucible coated with graphite. On the one hand, this change ensures that bubbles are generated evenly in all

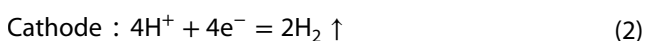
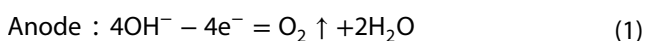
Fig.1 (a) Experiment setup with self-built thermostatic. (b) Schematic of the double-electrolyte etching method. (c) Photograph of self-designed tungsten wire clamping tool. (d) Orthographic views of the designed tungsten wire clamping tool



directions and will not aggregate to form larger bubbles which would affect the liquid level stability. On the other hand, the electrolysis of the stainless steel was avoided, which can produce metal ions and affect the etching process. Finally, a tungsten wire clamping tool was designed, as shown in Fig. 1c and d. This tool, which can hold various types of tungsten wires, is convenient to use. When a tip is fabricated, the same tungsten wire can be lowered down slightly for the next tip etching, without taking the wire out.

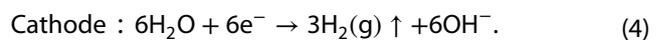
2.3 Double-electrolyte etching method

The principle of the double-electrolyte etching method is shown in Fig. 1b. The crucible is connected to the positive pole of the power supply as an anode, and the tungsten wire is in contact with a cathode. As the anode material is a stainless steel crucible coated with graphite, the electrolytic reaction of water occurs. The reaction equation can be expressed by:



Another electrolytic reaction is the electrochemical etching of the tungsten wire, where the wire plays the role

of the anode and the stainless steel ring is the cathode. The chemical reaction process can be expressed by:



The tungsten filament in the liquid lamellae becomes thinner when the electrochemical reaction is happening. Until gravity exceeds the tension that the neck can withstand, the lower end of the tungsten wire drops off, forming the upper and lower tips. Meanwhile, the circuit is automatically cut off to avoid further etching of tungsten tip.

2.4 Exploration on experimental parameters

Under the double-electrolyte etching method, other factors that may affect electrochemical etching reaction and tip quality were systematically explored:

Since the diameter of commercial STM probe holder is 0.3 mm and the matched tungsten wire has diameters of 0.2–0.25 mm, electrochemical etching experiments were carried out on two types of tungsten wires (diameter of 0.2 mm and 0.25 mm). Relatively, the most suitable and commonly used tungsten wire is 0.25 mm in diameter [33, 34, 36–38]. So the experiment of exploring optimal etching conditions was carried out with tungsten wires diameter

of 0.25 mm at different temperatures (20 °C, 23 °C, 26 °C and 29 °C), voltages (4 to 10V), electrolyte concentrations (1 to 5 mol L⁻¹) and lengths of tungsten wires below the liquid lamellae (2 to 9 mm). In addition, electrochemical etching experiments were also carried out with tungsten wires diameter of 0.2 mm, which aim to enrich the data of machine learning. The temperature was adjusted by the temperature control box.

3 Results and discussion

For this study, over 1900 tungsten tips were fabricated to eliminate the influence of other uncertainties as much as possible. And all the tip radius data in the experiment are calculated from the high-magnification SEM images to ensure accuracy. The average tip curvature radius, tip

aspect ratio and etching time under each set of conditions were calculated on average from ten sets of tip data.

3.1 Exploration of optimal etching condition

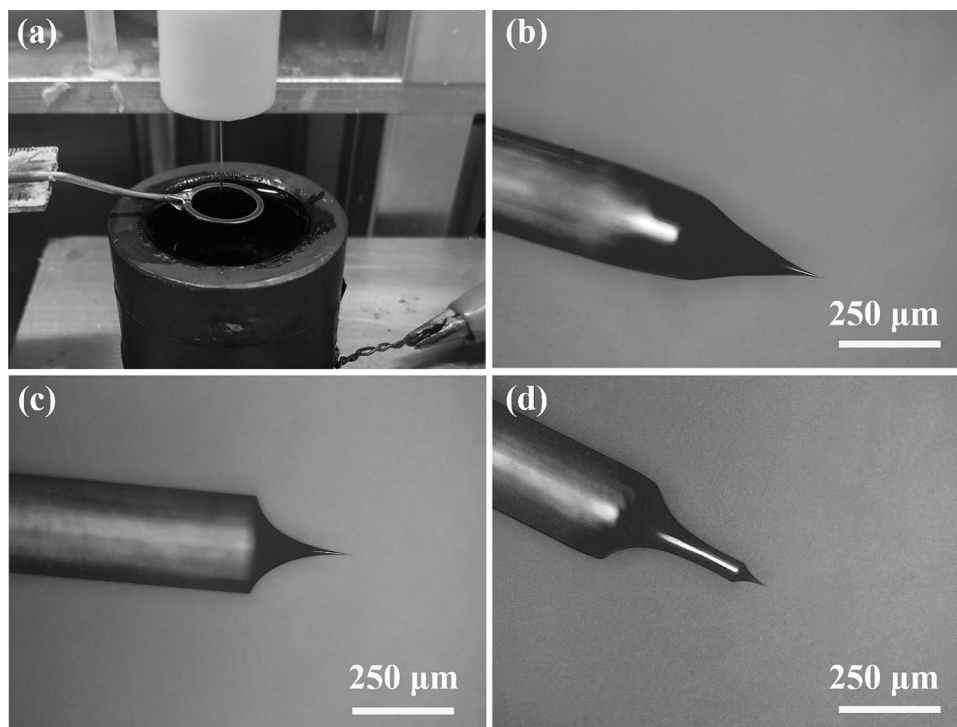
3.1.1 Influence of temperature on tip fabrication

Using the double-electrolyte etching method, the effects of temperature were studied. The temperature was set at 20 °C, 23 °C, 26 °C and 29 °C. And tungsten tips were fabricated under the following experimental conditions: electrolyte concentration of 3 mol L⁻¹, applied voltage of 8.5 V and tungsten wire length below the liquid lamellae of 7 mm. The etching time and the success rate for fabricating tungsten tips at different temperatures are shown in Table 1. When the temperature was 20 °C, it was too low to support the formation of liquid lamellae, as shown in Fig. 2a. And the experiment could not be performed.

Table 1 Statistics of tip etching time and fabrication success rate

Temperature (°C)	Applied voltage (V)	Electrolyte concentration (mol L ⁻¹)	Length below the liquid lamellae (mm)	Etching time ± 10 (s)	Success rate (%)
20	8.5	3	7	–	0
23	8.5	3	7	760	30
26	8.5	3	7	525	60
29	8.5	3	7	445	20

Fig.2 Images of the tips prepared by the double-electrolyte etching method at different temperatures: (a) 20 °C, (b) 23 °C, (c) 26 °C, (d) 29 °C



When the temperature was raised to 23 °C, although etching could be carried out, the etching time was so long that it risks lamellae rupture. The slow reaction rate at low temperature also made the formation of the “neck” incomplete, which resulted in an undesired tip shape as shown in Fig. 2b. For the temperature of 26 °C, both of the fabrication success rate and the tip shape improved. As shown in Fig. 2c, the shape of tungsten tip shows an ideal exponential curve which is preferred for quick and stable profile measurement during scanning [38]. A temperature of 29 °C was so high that there was an aggressive etching process which would break the liquid lamellae and make the etching position unstable. The tip fabricated under 29 °C shows a desirable multi-diameter profile (Fig. 2d), but the success rate dropped down to 20%. Thus, 26 °C was chosen as the most suitable temperature. Under such etching conditions, electrolyte concentration of 3 mol L⁻¹, applied voltage of 8.5 V, tungsten wire length below the

liquid lamellae of 7 mm and temperature of 26 °C, the average tip curvature radius is about 43 nm.

3.1.2 Influence of applied voltage on tip fabrication

During this series of tip fabrication, the effect of applied voltage on etching process was investigated. The temperature was set at 26 °C, the concentration of NaOH was 3 mol L⁻¹, the length of tungsten wire below the liquid lamellae was 7 mm, and the applied voltage was varied from 4 to 10 V. As illustrated in Fig. 3a and b, fabrication success rate above 70% can be achieved in the voltage range between 5 and 8 V. Voltages lower than 5 V made the etching time longer with increased risk of lamellae rupture. However, voltages higher than 8 V will cause violent vibration of bubbles and result in the rupture of the liquid lamellae. The high voltages will also produce multi-diameter tips, as Fig. 4 shows. Figure 3c and d shows the average curvature

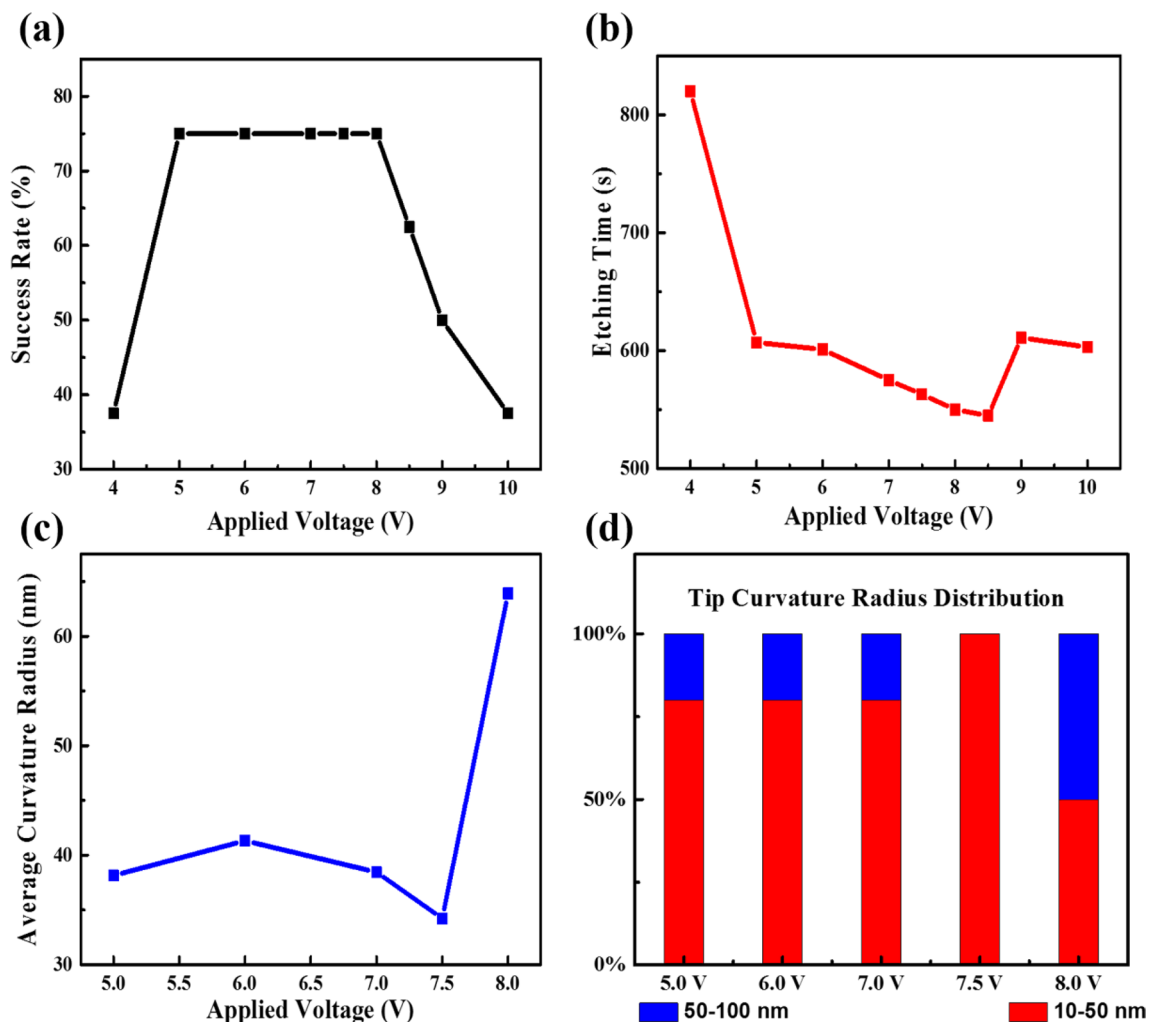


Fig.3 (a) Success rate of tip fabrication, (b) etching time of fabrication process, (c) tip average curvature radius and (d) tip curvature radius distribution under different applied voltages

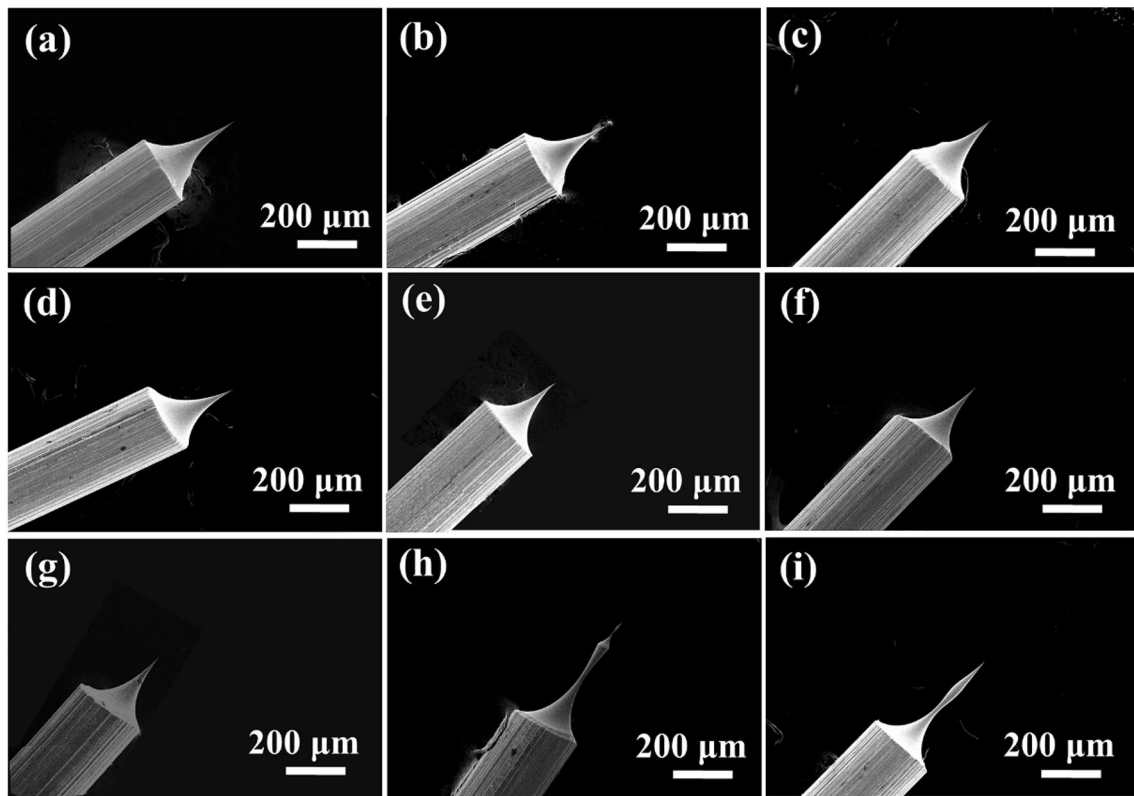


Fig.4 SEM images of tungsten tip fabricated at different voltages. (a), (b), (c), (d), (e), (f), (g), (h), (i) are voltages of 4 V, 5 V, 6 V, 7 V, 7.5 V, 8 V, 8.5 V, 9 V and 10 V, respectively

Table 2 Success rate of tip preparation and etching time under different electrolyte concentrations

Concentration (mol L ⁻¹)	Voltage (V)	Length (mm)	Etching time (s)	Success rate (%)
1	7.5	7	–	–
2	7.5	7	–	–
3	7.5	7	563	70
4	7.5	7	452	80
5	7.5	7	362	30

radius and the curvature radius distribution of the tungsten tips prepared under voltages of 5–8 V. The voltage of 7.5 V presents the smallest average tip curvature radius and the highest yield of tips between 10 and 50 nm. So, 7.5 V was selected as the most suitable applied voltage for the remaining study.

3.1.3 Influence of electrolyte concentration on tip fabrication

Based on the results in Sects. 3.1.1 and 3.1.2, a temperature of 26 °C, voltage of 7.5 V and a tungsten wire length

below the liquid lamellae of 7 mm were selected to study the effect of electrolyte concentration on tip fabrication. As listed in Table 2, five groups of electrolyte concentrations were selected from 1 to 5 mol L⁻¹. It was found that the electrolyte concentrations of 1 and 2 mol L⁻¹ could only produce a certain degree of neck shrinking without leading to tungsten wire drop-off to produce a tip (shown in Fig. 5). When the electrolyte concentration was raised up to 3 and 4 mol L⁻¹, the tip can have sufficient neck shrinking to form a tip. The fabrication success rate dropped to 30% as the electrolyte concentration increased to 5 mol L⁻¹, which is due to the bubble problem produced by the fast etching rate. When the concentration of electrolyte is 3 mol L⁻¹ and 4 mol L⁻¹, the success rate of tip fabrication is higher, and the etching time is much shorter than with the other concentrations. The statistical analysis of the tip curvature radius prepared by electrolyte concentrations of 3 and 4 mol L⁻¹ is listed in Table 3. Combining the tip average curvature radius and the distribution of tip curvature radius, 4 mol L⁻¹ was selected as the electrolyte concentration for the following studies.

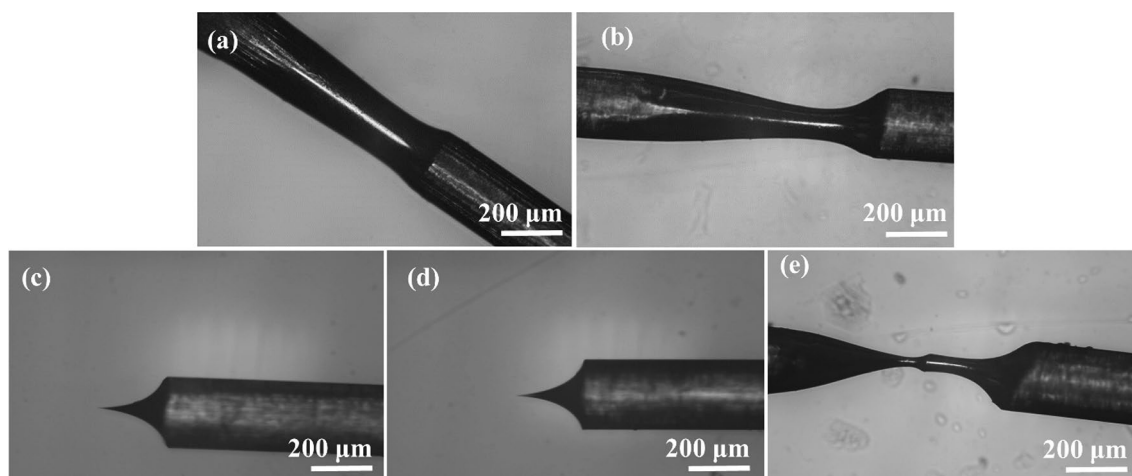


Fig.5 Tungsten wire obtained at different electrolyte concentrations: (a) 1 mol L⁻¹, (b) 2 mol L⁻¹, (c) 3 mol L⁻¹, (d) 4 mol L⁻¹, (e) 5 mol L⁻¹

Table 3 Curvature radius data of tip prepared at 3 mol L⁻¹ and 4 mol L⁻¹

Concentration (mol L ⁻¹)	Average curvature radius (nm)	Less than 10 nm (%)	10~20 nm (%)	20~50 nm (%)
3	34	0	0	100
4	32	0	20	80

3.1.4 Influence of the length of tungsten wire below the liquid lamellae on tip fabrication

Based on the above exploration, the temperature was set at 26 °C, the applied voltage was set at 7.5 V and the electrolyte concentration was set at 4 mol L⁻¹ to explore the influence of the length of tungsten wire below the liquid lamellae on tip preparation. Limited by the double lamellae method, the distance between the stainless steel ring and the lower crucible could not be too small; otherwise, the liquid lamellae and the solution in the lower crucible will overlap. In this experiment, the minimum tungsten wire length below the liquid lamellae is 2 mm. Figure 6 shows the statistical analysis of the tips fabricated under different lengths of tungsten wire. As shown in Fig. 6a and b, the etching time doesn't show significant variation by increasing the tungsten wire length below the liquid lamellae. Similarly, the success rate of tip fabrication was maintained above 80%, but dropped drastically for a wire length below the liquid lamellae greater than 8 mm. From Fig. 6c, with the increase in tungsten wire length below the liquid lamellae, the tip average curvature radius gradually increases, which can be interpreted by the fact that the excessively long tungsten filaments leads to the occurrence of "immature" drop-off. When 2 mm tungsten wire was immersed under the liquid lamellae, the etched tip

possessed the smallest average curvature radius and the yield of tip no more than 10 nm is 60% the highest yield between different lengths of tungsten wire below the liquid lamellae. To confirm the yield of tips less than 10 nm is as high as 60%, 200 additional tips were fabricated under the conditions of the length below the liquid lamellae of 2 mm. The distribution of tip radius is shown in Fig. 7. The radii of these 200 tips are all less than 50 nm and the yield of tip less than 10 nm increased to 63.5%, which may indicate that the larger sample size tends to make the preparation of the tip more stable. Figure 8 shows the SEM images of tips less than 10 nm fabricated under these conditions. Figure 8a and b shows the SEM images of tips with minimum curvature radius of about 8 nm. From further investigation of tip radius distribution, 2 mm was chosen as the optimal tungsten wire length below the liquid lamellae.

3.1.5 Tip performance under the optimized etching condition

From the above systematic etching experiments, the optimized etching conditions obtained are: temperature of 26 °C, applied voltage of 7.5 V, electrolyte concentration of 4 mol L⁻¹ and length below the liquid lamellae of 2 mm. Under such etching conditions, the smallest tip curvature radius is around 8 nm. The yield of tips less than 10 nm is 63.5%. Moreover, tungsten tips fabricated under the optimized etching conditions exhibited excellent detection performance working in STM. Figure 9 presents two topographic STM images of Si (111) surface and HOPG surface obtained at room temperature with these tips. The individual atoms of 7 × 7 reconstruction of Si (111) surface and the arrangement of two different positions of carbon atoms of HOPG surface were all clearly resolved, which can only be obtained by ultra-sharp tips.

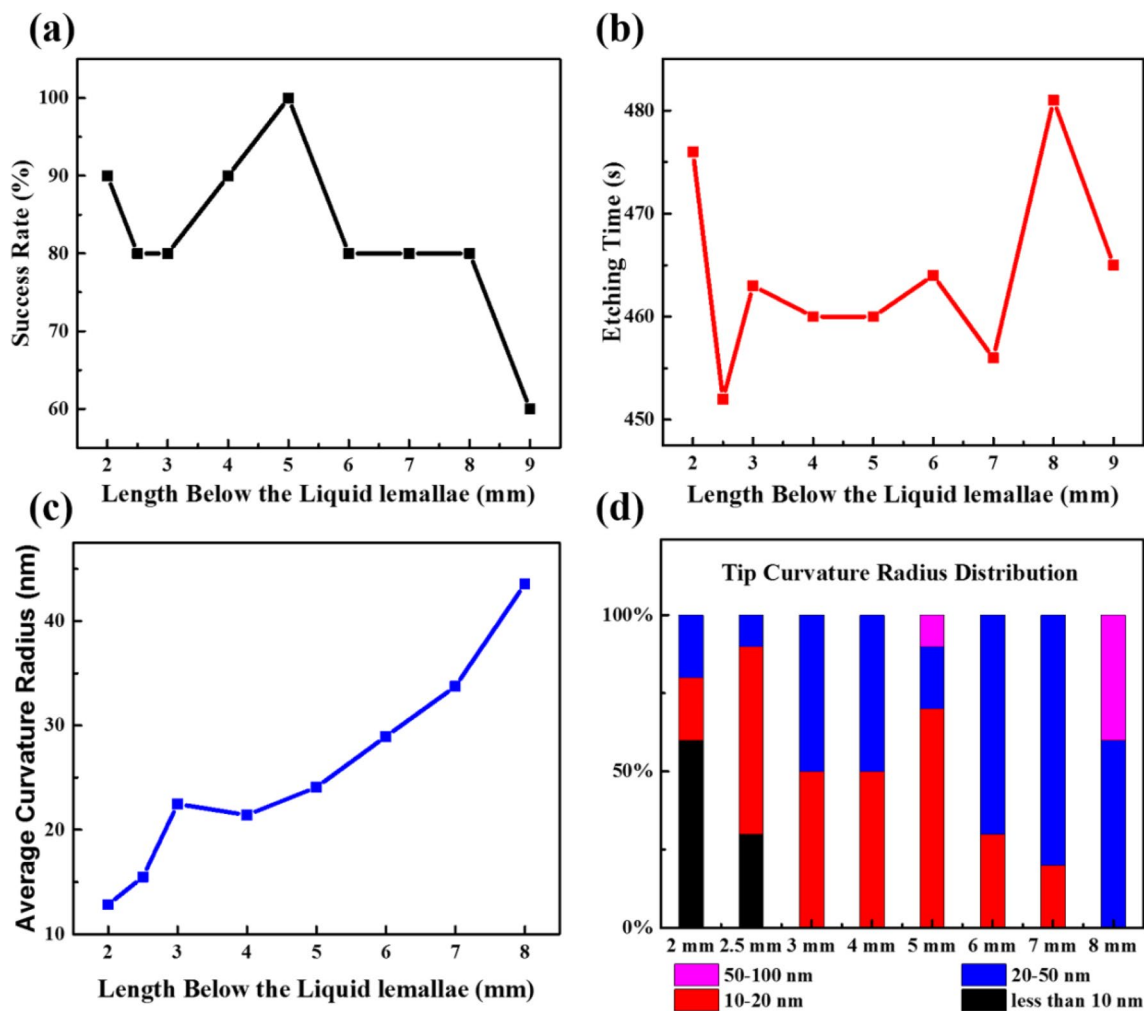


Fig.6 (a) Success rate of tip fabrication, (b) etching time of fabrication process, (c) tip average curvature radius and (d) tip curvature radius distribution under different lengths of tungsten wire below the liquid lamellae

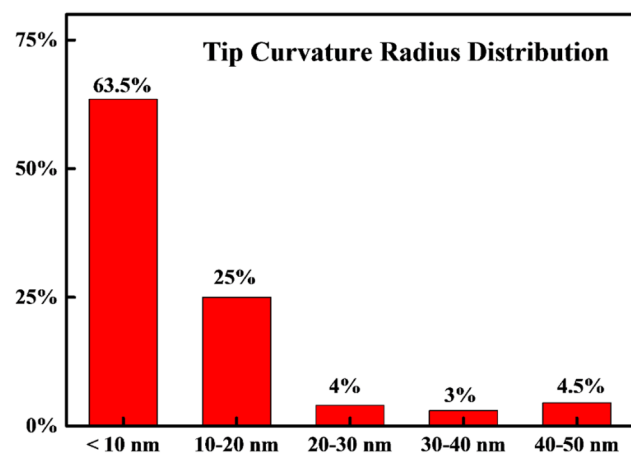


Fig.7 Tip curvature radius distribution under the length of tungsten wire below the liquid lamellae of 2 mm

3.2 Etching parameters importance analysis

ANN is one of the most effective machine learning methods [39]. By simulating the transmission process of human brain neurons, ANN can establish a large number of simple units that are known as neurons between input data and output data. Through continuously adjusting the interconnected weights between neurons and inputs or outputs, the mean square error between the network output and the actual value can reach the specified target accuracy, so as to realize the continuous approximation of the network output. Because of the fascinating features of self-learning and self-adaptation, ANNs are widely used in various fields to deal with complex and unknown function relations, such as biology [40], agriculture [41], engineering [42] and energy [43].

In this work, an ANN was employed to find the relationship between the tip features and etching parameters.

Fig.8 SEM images of tips fabricated under the optimized conditions: length of tungsten wire below the liquid lamellae of 2 mm, temperature of 26 °C, applied voltage of 7.5 V and electrolyte concentration of 4 mol L⁻¹

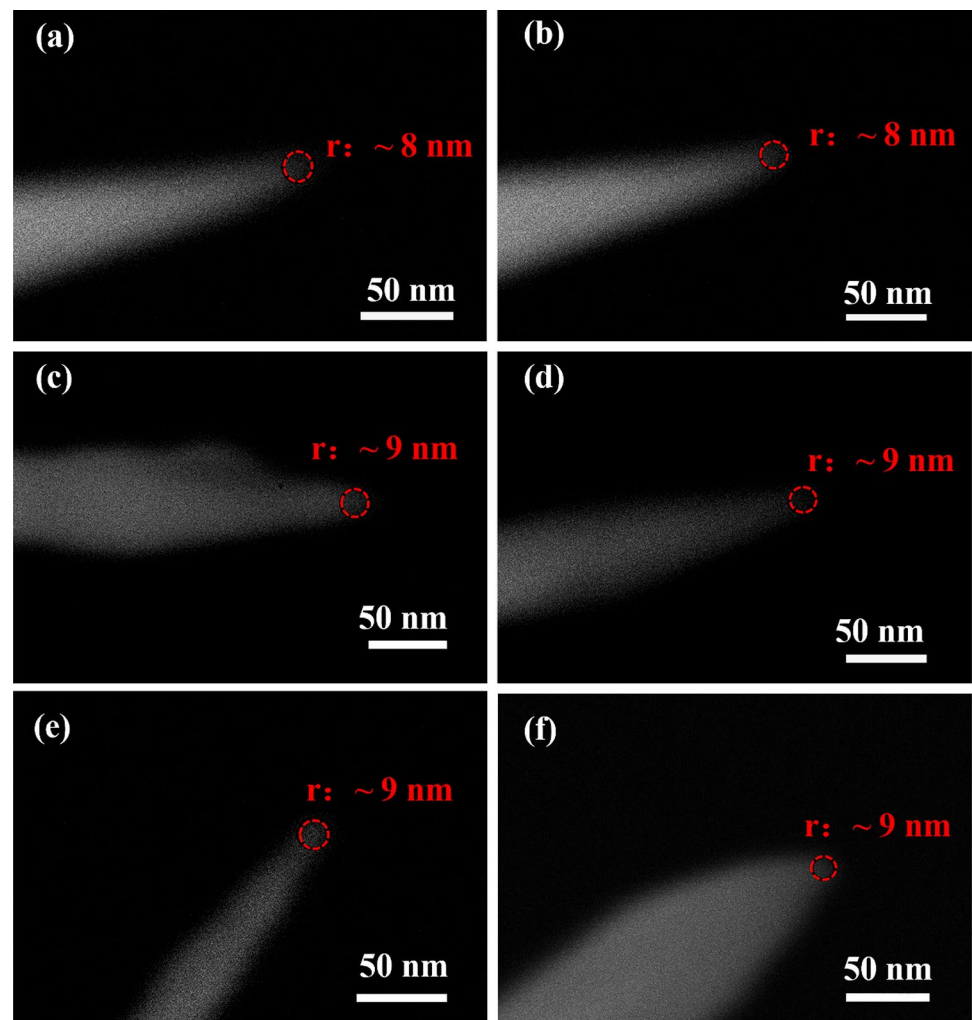
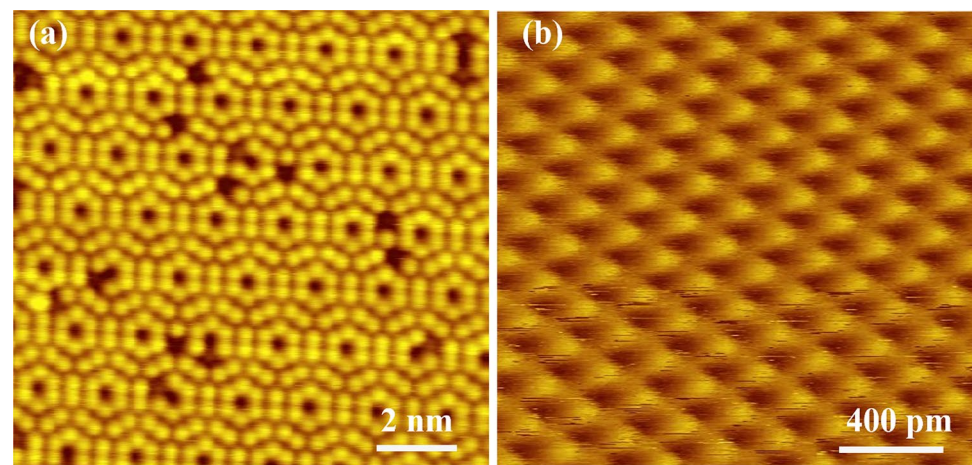


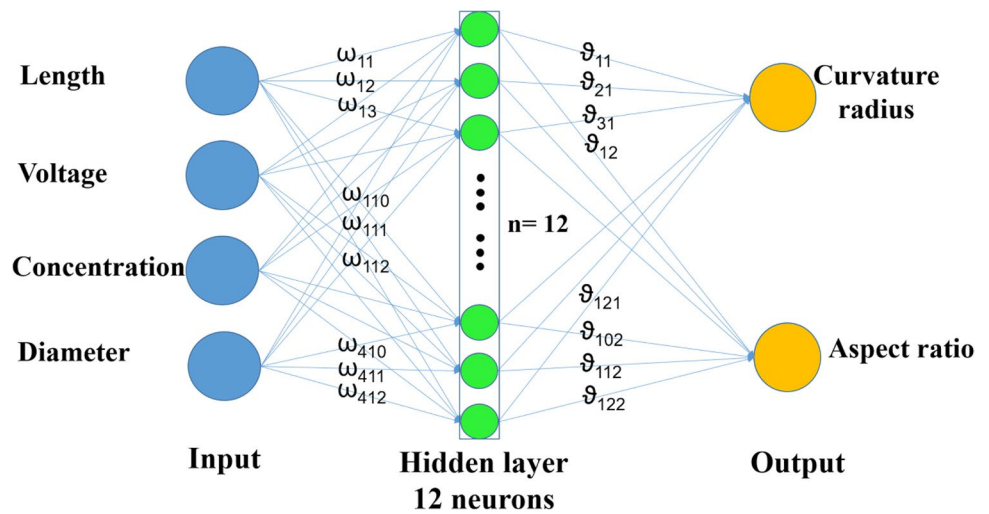
Fig.9 (a) STM image of Si (111) surface, image size is 15 × 15 nm, tunneling parameters are $V_b/I_t = 2.0 \text{ V} / 0.2 \text{ nA}$, room temperature. (b) STM image of HOPG surface, image size is 2 × 2 nm, tunneling parameters are $V_b/I_t = 0.366 \text{ V} / 0.5 \text{ nA}$, room temperature



Four parameters: the length of tungsten wire below the liquid lamellae, applied voltage, electrolyte concentration and tungsten wire diameter, were taken as the input units. Accordingly, the tip curvature radius and the tip

aspect ratio (the ratio of the etched length of the resulting tip to the diameter of the tungsten wire) were taken as the output units. An artificial neural network of 12 neurons at 3 layers was established by a MATLAB program.

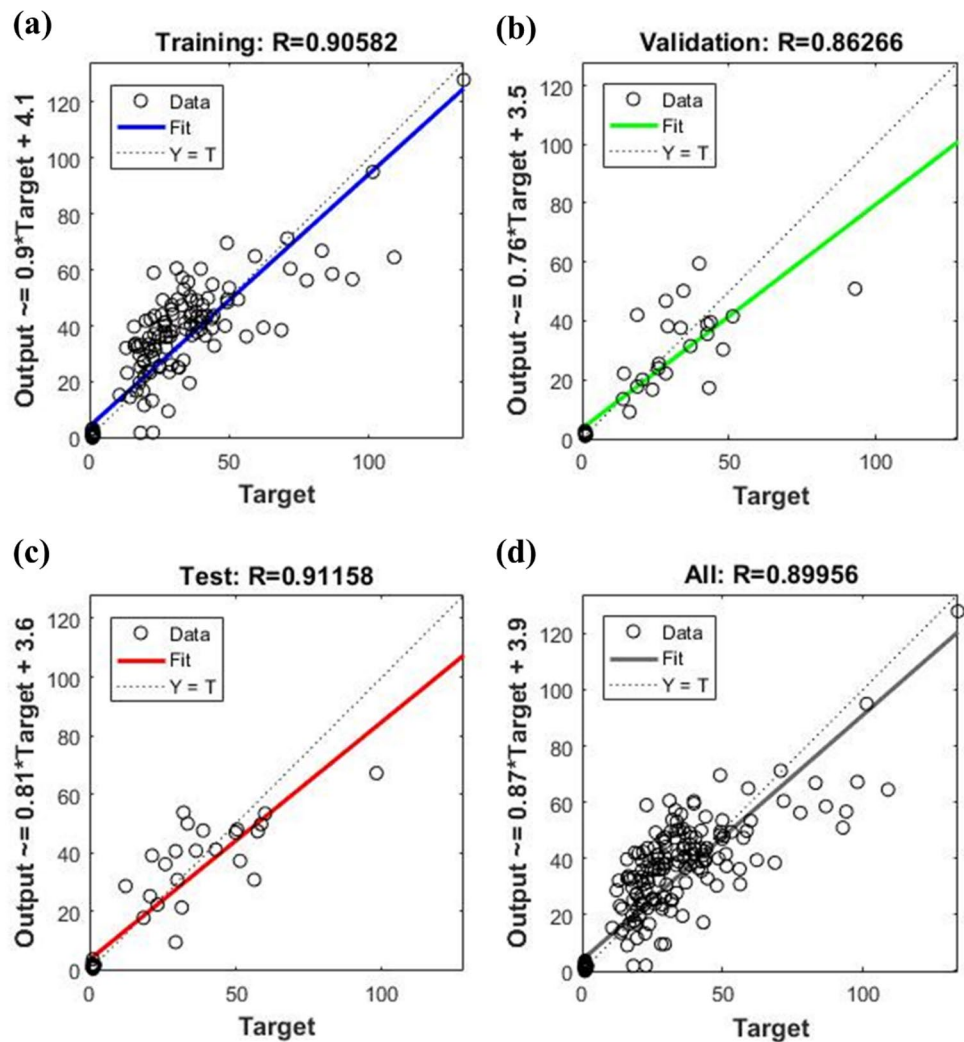
Fig.10 Architecture of artificial neural network



The architecture of this ANN is illustrated in Fig. 10. In order to train a good ANN model, 157 groups of etching parameters were input into the MATLAB program. These

data were randomly classified into three parts: training, validation and test, which were used for model establishment, confirmation and prediction accuracy test,

Fig.11 Regression of predicted data to experiment data. (a) Regression of predicted data to training data. (b) Regression of predicted data to validation data. (c) Regression of predicted data to test data. (d) Regression of predicted data to all experimental data. (For a perfect fit, the 45-degree line ($Y = T$), where the network outputs are equal to the targets, represents the most perfect fit.)



respectively. Figure 11a, b and c displays the regression chart of network outputs (predicted data) with respect to targets (experimental data) for training, validation and test sets. Figure 11d shows the regression of predicted data obtained from intelligent model of ANN to all the input experimental data. The R value which measures the correlation between predicted data and experimental data is used to evaluate the fitting performance of ANN models. An R of 1 means a very close relationship; 0 is a random relationship. As shown in Fig. 11, the correlation factors (R) are all over 0.85, which represents a great fit. The attractive property of ANN is to make learning-based predictions. Here, this ANN model was used to predict curvature radii and aspect ratios of 8 tips fabricated at new experimental conditions to test the predictive performance. The predicted results are illustrated in Fig. 12. It is found that the general trends of predicted values are consistent with the experimental ones. Specially, several predicted values are the same as the experimental ones, which means that the model made by ANN can give a credible guidance predicting tip features under different experimental conditions.

In the experiment of preparing tungsten tips by double-electrolyte etching method, the optimal etching conditions may have some deviation due to different experimental conditions in different laboratories. In this case, the weight analysis of each experimental parameter on the tip feature is more meaningful, which can help researchers quickly find optimized experimental parameters. Garson's algorithm is a sensitivity analysis method for obtaining the weight of influence factors by means of neural network [44]. In this algorithm, the product of interconnected weights is used to calculate the influence degree or relative contribution value of input variables on output variables. After repeated testing and training of Garson's

algorithm by researchers, a mature formula was obtained and widely applied. The specific calculation formula is shown in Eq. (5) [45]:

$$Q_{ik} = \frac{\sum_{j=1}^L \frac{|\omega_{ij}\vartheta_{jk}|}{\sum_{i=1}^N |\omega_{ij}|}}{\sum_{i=1}^N \sum_{j=1}^L \frac{|\omega_{ij}\vartheta_{jk}|}{\sum_{i=1}^N |\omega_{ij}|}} \times 100\%, \quad (5)$$

$$(l = 1, \dots, N; j = 1, \dots, L).$$

where Q_{ik} denotes the weight of the i th input factor on the k th output factor, ω_{ij} denotes the interconnected weights between the i th input unit and the j th neuron and ϑ_{jk} denotes the interconnected weights between the j th neuron and the k th output unit.

For this ANN mode, Garson's algorithm was used to calculate the relative importance of each parameter. Table 4 lists the interconnected weights of neurons in input, neuron and output. The weight of each factor on the tip features is obtained with the data of Table 4 into Eq. (5) and shown in Fig. 13. This importance analysis shows that the length of the tungsten wire below the liquid lamellae is the most important factor, followed by applied voltage. In contrast, the electrolyte concentration and tungsten wire diameter have little effect on tip quality in the double-electrolyte etching method.

4 Conclusions

The double-electrolyte etching method was applied to synthesize ultra-sharp tungsten STM tips and enhance their yield. Adding a control box to stabilize the temperature allowed a systematic study to obtain optimized

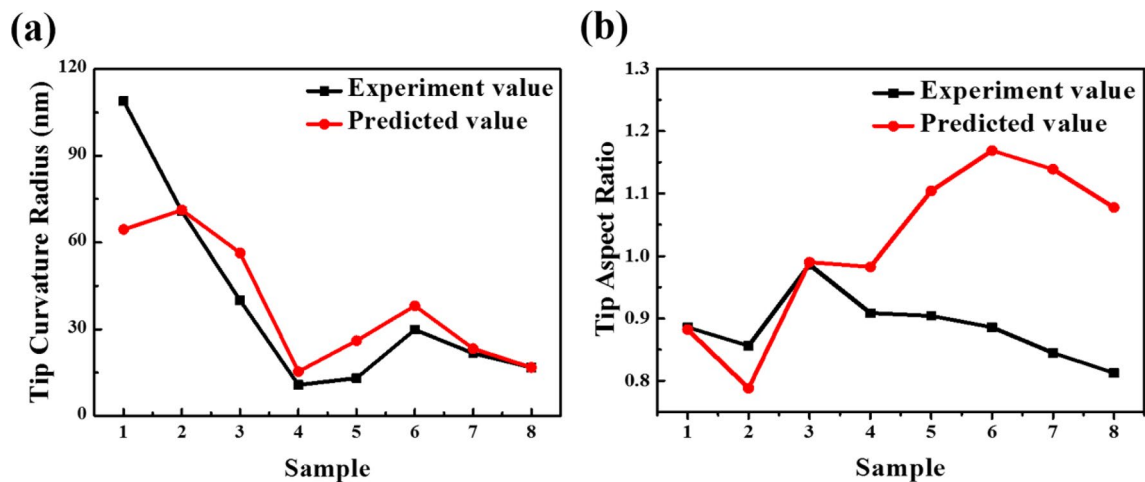


Fig. 12 (a) Prediction result by ANN and the experimental data of tip radius, (b) prediction result by ANN and the experimental data of tip aspect ratio

Table 4 Interconnected weights between neurons and inputs or outputs^a

	I1	I2	I3	I4	O1	O2
N 1	−1.83	0.18	0.07	−0.02	−1.58	0.21
N 2	2.12	−4.30	−1.46	−3.63	0.34	0.16
N 3	3.18	−2.86	−0.24	−0.76	−0.58	0.05
N 4	4.14	1.25	0.74	−0.32	−0.64	0.13
N 5	−1.65	−2.29	−0.81	1.04	−0.53	0.09
N 6	−1.50	3.29	−0.80	−0.78	−0.45	−0.01
N 7	1.86	−1.72	−1.33	1.98	1.22	0.08
N 8	2.38	−1.93	0.51	3.30	−0.93	0.01
N 9	0.32	−2.20	−2.90	0.78	−0.29	0.03
N 10	1.30	−0.82	−0.59	−1.02	−1.58	−0.13
N 11	1.18	4.04	0.24	−0.94	0.24	0.05
N 12	−1.49	−0.28	−0.74	0.90	−0.12	−0.17

^aN1–N12: neuron 1–neuron 12; I1: input 1—length of tungsten wire below the liquid lamellae; I2: input 2—applied voltage; I3: input 3—electrolyte concentration; I4: input 4—diameter of tungsten wire; O1: output 1—tip curvature radius; O2: output 2—tip aspect ratio.

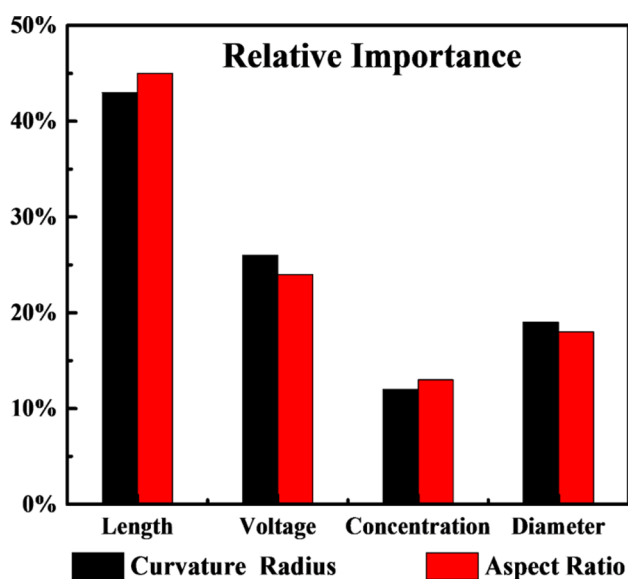


Fig. 13 Relative importance of etching parameters to tip features. Length: length of tungsten wire below the liquid lamellae. Voltage: applied voltage. Concentration: electrolyte concentration. Diameter: tungsten wire diameter

electrochemical etching parameters. Under these conditions, the smallest curvature radius is around 8 nm; the yield of ultra-sharp tungsten tips with the curvature radii below 10 nm is 63.5%. Such tungsten tips have been stably used to obtain high-quality STM images with atomic resolution, which were demonstrated with Si and HOPG samples. Furthermore, by using ANN and Garson's algorithm, the tip features are well predicted and the relative importance of four tip etching parameters was obtained. The length of tungsten wire below the liquid lamellae was regarded as the most important factor in the

double-electrolyte etching method, followed by applied voltage, the diameter of tungsten wire and electrolyte concentration.

Acknowledgements This work was financially supported by the National Nature Science Foundation of China (No. 11774255) and the Key Project of Natural Science Foundation of Tianjin City (No. 17JCZDJC30100).

Compliance with ethical standards

Conflict of interest The co-authors declare that they have no conflict of interest in this manuscript.

References

- Gu H, Zhang H, Ma C, Sun H, Liu C, Dai K, Zhang J, Wei R, Ding T, Guo Z (2019) Smart strain sensing organic–inorganic hybrid hydrogels with nano barium ferrite as the cross-linker. *J Mater Chem C* 7(8):2353–2360
- Nasiri H, Jamalabadi MYA, Sadeghi R, Safaei MR, Nguyen TK, Shadloo MS (2019) A smoothed particle hydrodynamics approach for numerical simulation of nano-fluid flows. *J Therm Anal Calorim* 135(3):1733–1741
- Cai Y, Wei Z, Song C, Tang C, Han W, Dong X (2019) Optical nano-agents in the second near-infrared window for biomedical applications. *Chem Soc Rev* 48(1):22–37
- Bottomley LA, Chem A (1998) Scanning probe microscopy. *Anal Chem* 68(12):185–230
- Dulub O, Boatner LA, Diebold U (2002) STM study of the geometric and electronic structure of ZnO(0 0 0 1)–Zn, (0 0 0 1 $\bar{1}$)–O, (1 0 1 $\bar{1}$ 0), and (1 1 2 $\bar{1}$ 0) surfaces. *Surf Sci* 519(3):201–217
- Aleman M, Peters MV, Hecht S, Rieder KH, Moresco F, Grill L (2006) Electric field-induced isomerization of azobenzene by STM. *J Am Chem Soc* 128(45):14446–14447
- Houel A, Tonneau D, Bonnail N, Dallaporta H (2002) Direct patterning of nanostructures by field-induced deposition from

- a scanning tunneling microscope tip. *J Vacuum Sci Technol B Microelectron Nanometer Struct* 20(6):2337–2345
8. Shi Q, Huang D, Zhu Q (2014) Vibrational-energy redistribution in single-atom manipulation by scanning tunneling microscope. *Jpn J Appl Phys* 38(6B):3856–3859
 9. Binnig G, Rohrer H, Gerber C, Weibel E (1993) Surface studies by scanning tunneling microscopy. In: Neddermeyer H (ed) *Scanning tunneling microscopy*. Springer, Dordrecht, pp 31–35
 10. Hofer WA, Foster AS, Shluger AL (2003) Theories of scanning probe microscopes at the atomic scale. *Rev Mod Phys* 75(7):1287–1331
 11. Revenikiotis SA (2011) Optimization of STM-tip preparation methods
 12. Melmed AJ (1991) The art and science and other aspects of making sharp tips. *J Vacuum Sci Technol B* 9(2):601–608
 13. Ibe JP, Bey PP, Brandow SL, Brizzolara RA (1990) On the electrochemical etching of tips for scanning tunneling microscopy. *J Vacuum Sci Technol Vacuum Surf Films* 8(4):3570–3575
 14. Nakamura Y, Mera Y, Maeda K (1999) A reproducible method to fabricate atomically sharp tips for scanning tunneling microscopy. *Rev Sci Instrum* 70(8):3373–3376
 15. Zhang R, Ivey DG (1996) Preparation of sharp polycrystalline tungsten tips for scanning tunneling microscopy imaging. *J Vacuum Sci Technol B Microelectron Nanometer Struct Process Meas Phenom* 14(1):1–10
 16. Kim YG, Choi EH, Kang SO, Cho G (1998) Computer-controlled fabrication of ultra-sharp tungsten tips. *J Vacuum Sci Technol B Microelectron Nanometer Struct Process Meas Phenom* 16(4):2079–2081
 17. Fainchtein R, Zariello PR (1992) A computer-controlled technique for electrochemical STM tip fabrication. *Ultramicroscopy* 42–44(3):1533–1537
 18. Ge Y, Zhang W, Chen YL, Jin C, Ju BF (2013) A reproducible electropolishing technique to customize tungsten SPM probe: From mathematical modeling to realization. *J Mater Process Tech* 213(1):11–19
 19. Chen Y, Xu W, Huang J (2000) A simple new technique for preparing STM tips. *J Phys E Sci Instrum* 22(7):455–457
 20. Kim DI, Ahn HS (2002) Etching voltage control technique for electrochemical fabrication of scanning probe microscope tips. *Rev Sci Instrum* 73(3):1337–1339
 21. Musselman IH, Peterson PA, Russell PE (2015) Fabrication of tips with controlled geometry for scanning tunnelling microscopy. *Precis Eng* 12(1):3–6
 22. Chang WT, Hwang IS, Chang MT, Lin CY, Hsu WH, Hou JL (2012) Method of electrochemical etching of tungsten tips with controllable profiles. *Rev Sci Instrum* 83(8):3570
 23. Tahmasebipour G, Hojjat Y, Ahmadi V, Abdullah A (2009) Optimization of STM/FIM nanotip aspect ratio based on the Taguchi method. *Int J Adv Manuf Technol* 44(1–2):80–90
 24. SL A (2004) Preparation and characterization of tungsten tips suitable for molecular electronics studies. McGill University
 25. Knápek A, Sýkora J, Chlumská J, Sobola D (2017) Programmable set-up for electrochemical preparation of STM tips and ultra-sharp field emission cathodes. *Microelectron Eng* 173(173):42–47
 26. Guise OL, Ahner JW, Jung M-C, Goughnour PC, Yates JT (2002) Reproducible electrochemical etching of tungsten probe tips. *Nano Lett* 2(3):191–193
 27. Bernal R, Ávila A (2008) Reproducible fabrication of scanning tunneling microscope tips. *Revista de Ingeniería* 27:43–48
 28. Song J, Pryds N, Glejbo LK, Morch K, Thölen A, Christensen LN (1993) A development in the preparation of sharp scanning tunneling microscopy tips. *Rev Sci Instrum* 64(4):900–903
 29. Wang Y, Zeng Y, Wang X, Qu N, Zhu D (2016) Liquid membrane electrochemical etching: twin nano-tips fabrication for micromachining. *Int J Electrochem Sci* 11:4174–4185
 30. Lemke H, Göddenhenrich T, Bochem HP, Hartmann U, Heiden C (1990) Improved microtips for scanning probe microscopy. *Rev Sci Instrum* 61(10):2538–2541
 31. Klein M, Schwitzgebel G (1997) An improved lamellae drop-off technique for sharp tip preparation in scanning tunneling microscopy. *Rev Sci Instrum* 68(8):3099–3103
 32. Kulawik M, Nowicki M, Thielsch G, Cramer L, Rust HP, Freund HJ, Pearl TP, Weiss PS (2003) A double lamellae dropoff etching procedure for tungsten tips attached to tuning fork atomic force microscopy/scanning tunneling microscopy sensors. *Rev Sci Instrum* 74(2):1027–1030
 33. Schoelz JK, Xu P, Barber SD, Qi D, Ackerman ML, Basnet G, Cook CT, Thibado PM (2012) High-percentage success method for preparing and pre-evaluating tungsten tips for atomic-resolution scanning tunneling microscopy. *J Vacuum Sci Technol B Microelectron Nanometer Struct* 30(3):033201–033201-5
 34. Basnet G, Kevin Schoelz J, Xu P, Barber SD, Ackerman ML, Thibado PM (2013) Etch-stop method for reliably fabricating sharp yet mechanically stable scanning tunneling microscope tips. *J Vacuum Sci Technol B Nanotechnol Microelectron Mater Process Meas Phenom* 31(4):043201
 35. Li Y, Song Z, Zhang Y, Wang Z, Xu Z, Lin R, Qian J (2019) A double-electrolyte etching method of high-quality tungsten probe for undergraduate scanning tunneling microscopy and atomic force microscopy experiments. *Eur J Phys* 40:025004
 36. Ju B-F, Chen Y-L, Fu M, Chen Y, Yang Y (2009) Systematic study of electropolishing technique for improving the quality and production reproducibility of tungsten STM probe. *Sens Actuators A Phys* 155(1):136–144
 37. Derouin J, Farber RG, Thaker AA, Valencia V (2015) Preparation of scanning tunneling microscopy tips using pulsed alternating current etching. *J Vacuum Sci Technol Vacuum Surf Films* 33(2):023001
 38. Ju BF, Chen YL, Ge Y (2011) The art of electrochemical etching for preparing tungsten probes with controllable tip profile and characteristic parameters. *Rev Sci Instrum* 82(1):2359
 39. Wang J, Li Z, Yan S, Yu X, Ma L (2019) Modifying the microstructure of algae-based active carbon and modelling supercapacitors using artificial neural networks. *RSC Adv* 9(26):14797–14808
 40. Shi Y, Wang G, Niu J, Zhang Q, Cai M, Sun B, Wang D, Xue M, Zhang XD (2018) Classification of sputum sounds using artificial neural network and wavelet transform. *Int J Biol Sci* 14(8):938–945
 41. Tan J, Kerr WL (2018) determining degree of roasting in cocoa beans by artificial neural network (ANN) based electronic nose system and gas chromatography/mass spectrometry (GC/MS). *J Sci Food Agric* 98:3851–3859
 42. Selvan SS, Pandian PS, Subathira A, Saravanan S (2018) Comparison of response surface methodology (RSM) and artificial neural network (ANN) in optimization of aegle marmelos oil extraction for biodiesel production. *Arab J Sci Eng* 2:1–13
 43. Dong S, Zhang Y, He Z, Na D, Yu X, Sheng Y (2018) Investigation of support vector machine and back propagation artificial neural network for performance prediction of the organic Rankine cycle system. *Energy* 144:851–864
 44. Garson GD (1991) Interpreting neural network connection weights. *Ai Expert* 6(4):46–51
 45. Sun M, Ji L (2017) In: Improved Garson algorithm based on neural network model, Chinese Control & Decision Conference

Publisher's Note Springer Nature remains neutral with regard to jurisdictional claims in published maps and institutional affiliations.